

Metallic resistivity in crystalline ropes of single-wall carbon nanotubes

J. E. Fischer,¹ H. Dai,² A. Thess,² R. Lee,¹ N. M. Hanjani,¹ D. L. Dehaas,¹ and R. E. Smalley²

¹*Department of Materials Science and Engineering and Laboratory for Research on the Structure of Matter,*

University of Pennsylvania, Philadelphia, Pennsylvania 19104-6272

²*Center for Nanoscale Science and Technology, Rice Quantum Institute*
and Departments of Chemistry and Physics, Rice University, Houston Texas 77251

(Received 3 September 1996)

Laser ablation of (Co,Ni)-doped graphite yields $\sim 70\%$ single-wall nanotubes, predominantly (10,10) armchair tubes which self-organize into crystalline "ropes" $>100 \text{ \AA}$ in diameter and $>10 \mu\text{m}$ long. We find $\rho_{\parallel} = 0.03\text{--}0.10 \text{ m}\Omega \text{ cm}$ at 300 K, with positive (negative) $d\rho/dT$ above (below) $T^* = 35 \text{ K}$. Unoriented bulk samples exhibit similar behavior, with higher (directionally averaged) resistivities and T^* 's. The high- T behavior is consistent with the predicted intrinsic metallic state for this structure. [S0163-1829(97)51604-3]

Carbon nanotubes are attracting increasing scientific and technological interest.¹ Defect-free tubes are expected to have electronic and magnetic properties which depend on the diameter, number of concentric shells, and chirality. Active devices based on diameter discontinuities within a single tube are also envisioned.²

Several groups have reported electrical resistivity results for multiwall nanotubes (MWNT's). Oriented films of MWNT's provided the first determination of the resistivity along the tube axis, $\rho_{\parallel} \sim 20 \text{ m}\Omega \text{ cm}$ at 300 K, increasing gradually with decreasing temperature.³ Two-probe magnetoconductivity measurements on individual MWNT's show evidence for weak localization.⁴ Scanning probe⁵ and four-probe⁶ resistivity values at 300 K span four decades, no doubt reflecting the influence of defects as well as different diameters, number of shells, etc. Despite the low resistivities sometimes found, none of the MWNT samples show the positive $d\rho/dT$ characteristic of a metal.

Single-wall nanotubes (SWNT's) are conceptually simpler, having only one structural degree of freedom since diameter and chirality are interdependent. The electronic spectrum is completely specified by the integer pair (n,m) which also defines the structure. SWNT's with $n=m$ or $m=0$ are achiral, having, respectively, "armchair" or "zigzag" configurations of carbon atoms in planes normal to the tube axis. Starting from the zero-gap electron spectrum of an infinite graphene sheet, and depending on the choice of n and m , primary (large) and secondary (small) gaps may be opened by zone folding and curvature, respectively; one thus finds that only SWNT's with $n=m$ have gapless densities of states and therefore should be metallic.⁷⁻⁹

It has been shown recently that essentially monodisperse SWNT's are produced, in yields approaching 70%, by laser ablation of graphite doped with Co and Ni.^{10,11} Armchair tubes are predicted to be energetically favored due to effective triple bond formation on the open edge during growth.¹¹ X-ray diffraction and transmission electron microscopy (TEM) lattice images¹¹ provide strong evidence that the (10,10) armchair tube with a measured diameter of $13.8 \pm 0.2 \text{ \AA}$ is predominant. The armchair geometry was specifically confirmed by electron diffraction¹² and Raman spectroscopy.¹³ Therefore, this material is expected to be me-

tallic. Amazingly, the SWNT's self-organize during growth into bundles, or ropes, tens of micrometers long, containing hundreds of close-packed tubes on a two-dimensional (2D) triangular lattice with intertube spacing 3.2 \AA characteristic of van der Waals inter-SWNT binding.¹¹ Thus the anisotropy of rope electronic properties should resemble that of graphite, while individual SWNT's might be viewed as 1D quantum wires or electron waveguides.

Evidence that the ropes are metallic include a Dysonian electron-spin resonance spectrum with $g=2.001$, ρ_{\parallel} for several single-rope samples falling in a narrow range $0.03\text{--}0.1 \text{ m}\Omega \text{ cm}$ (straddling the in-plane resistivity of graphite,¹⁴ $0.04 \text{ m}\Omega \text{ cm}$), and positive $d\rho/dT$, all at or near 300 K (Ref. 11). Here we present $\rho_{\parallel}(T)$ and $\langle\rho\rangle(T)$ data from individual ropes and unoriented bulk samples, or mats, of long tangled ropes, respectively. The results are strikingly similar. At high temperature we observe $\rho(T)$ increasing linearly with T in single ropes and in mats subjected to different thermal and mechanical treatments. This behavior changes with decreasing temperature to *negative* $d\rho/dT$, with low- T slopes and crossover temperatures T^* varying from sample to sample. In contrast to this near-universal behavior, mat samples with demonstrably lower yield of SWNT's have $d\rho/dT < 0$ up to at least 500 K, similar to published data for MWNT's samples. We believe that the positive $d\rho/dT$ confirms the predicted intrinsic metallic nature of (10,10) SWNT's, and that the relative purity and perfection of the material studied allows this to be observed, unobscured by the effects of defects and disorder. We are less certain of the origin of the negative $d\rho/dT$ at low T ; a speculation is presented and experimental tests suggested.

Samples produced by the laser ablation process consist of fairly robust, uniformly thick mats, diffuse black in reflection and with macroscopic densities of only a few mg/cm^3 , which condense on a water-cooled Cu surface. As produced, these contain C_{60} , C_{70} , and microcrystalline Co and Ni catalyst residues along with the SWNT's. No MWNT's are observed in TEM or powder x-ray diffraction. The fullerenes and much of the Co and Ni are removed by heat treatment in vacuum or inert gas at 1000°C for 30 min.¹¹ Four-probe ρ_{\parallel} measurements were performed at ambient temperature by extracting a single rope from the mat using a sharpened Pt tip

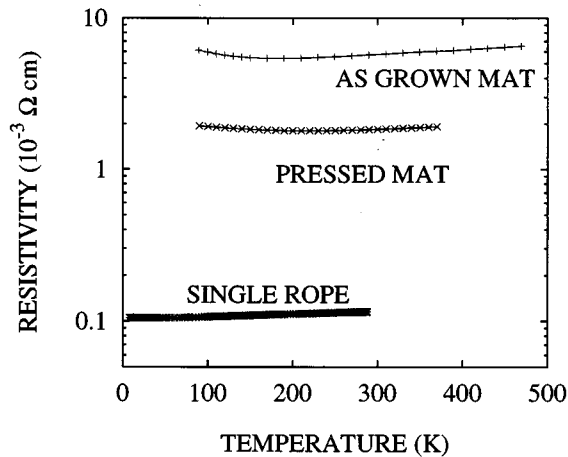


FIG. 1. Resistivity vs temperature for SWNT rope materials: as-grown and lightly pressed mat (four-point, unoriented) and single-rope (two-point, scaled to four-point measurement at ambient T). Solid curves are guides to the eye.

and two MWNT's as voltage probes and measuring the rope diameter in the TEM.¹¹ The highest of these values, 0.1 m Ω cm, was used to scale the results of two-point single-rope resistance vs T measured in a standard He cryostat to give the lower curve in Fig. 1.

Four-point measurements of the directionally averaged bulk resistivity $\langle\rho\rangle$ were made on rectangular pieces 2–4 mm wide and \sim 1 cm long, cut from the mat. Resistivities were calculated using an average thickness estimated from the mass (100's of μ g) and an assumed density 2 g/cm³, intermediate between solid C₆₀ and graphite. We used in-line silver paint or pressure contacts and high-pressure Ar in a Joule-Thompson cold finger cryostat¹⁵ which can be heated to 580 K. $\langle\rho\rangle$ of as-grown mat annealed at 1000 °C is shown as the upper curve in Fig. 1. We find it remarkable that $\langle\rho\rangle$ (mat) exceeds ρ_{\parallel} (rope) by only a factor \sim 50 since the inter-rope contacts in the mat must be tenuous at best in light of the extremely low density, and since we expect $\rho_{\perp}\gg\rho_{\parallel}$ as in graphite.^{14,16} We suspect that the relatively small difference between $\langle\rho\rangle$ and ρ_{\parallel} can be explained by the extreme aspect ratio of the ropes comprising the mat; the length of the rope segments is an appreciable fraction of the length between voltage probes¹⁷ such that the number of rope-rope contacts is far less than usually encountered in powder pellets. Evidence that this is indeed the case is provided by the middle curve in Fig. 1, showing that mild pressing of the mat before applying contacts (4 kg/cm²) permanently reduces $\langle\rho\rangle$ by a factor 3, the improved rope-rope contact bringing the mat value within a factor 20 of ρ_{\parallel} . By systematically increasing the pressing force, we found a shallow minimum in $\langle\rho\rangle$ at 6 kg/cm²; increasing further to 8 kg/cm² led to a twofold increase in $\langle\rho\rangle$. The highest pressure apparently signals the point at which mechanical damage to the ropes or tubes comprising the mat overtakes the improvement in rope-rope contacts.

Figure 2 displays the temperature dependence on an expanded relative scale. Above T^* , both ρ_{\parallel} and $\langle\rho\rangle$ are fairly well described by positive linear coefficients, 0.52×10^{-4} /K

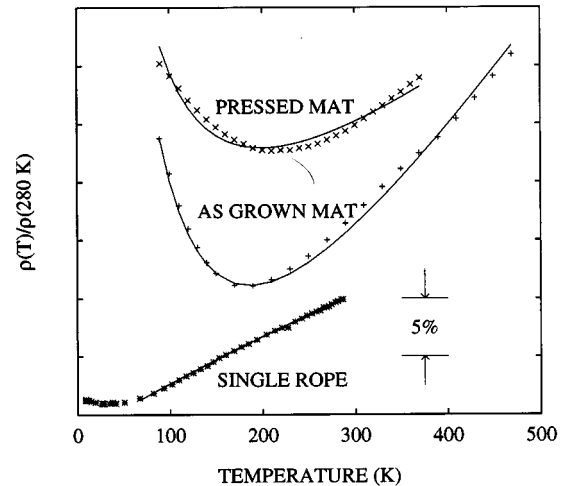


FIG. 2. Resistivity vs temperature (normalized to 300 K) of SWNT single rope (ρ_{\parallel}) and mat ($\langle\rho\rangle$). All samples show a crossover from positive to negative $d\rho/dT$, at different temperatures. For clarity, the curves are offset and two of every three single-rope data points are omitted. Solid curves are fits described in the text.

for the single rope and $\sim 1\times 10^{-4}$ /K for the as-grown mat. The derivative changes sign at low T , the crossover temperature T^* increasing from 35 K to 180 K to 210 K in the sequence rope < as-grown mat < pressed mat. The mat data can be approximately fit by $\rho=A+B/T+CT$ with considerable uncertainty in the exponent of the $1/T$ term, while the single-rope data above 50 K are well represented by $A+CT-DT^2$, the negative quadratic coefficient perhaps suggesting the onset of saturation.

Both the positive $d\rho/dT$ at high T and the crossover phenomenon are robust in high-yield mats; for example increasing the annealing time and temperature to 30 h at 1200 °C simply increases $\langle\rho\rangle$ by 25% at all T , and compression has little effect on T^* . Conversely, low-yield mat samples (resulting from less-than-optimum matching conditions of the two laser beams) give significantly higher $\langle\rho\rangle$, and $d\rho/dT<0$ from 90 K to 500 K similar to the behavior of MWNT's.^{3,4,6} Further evidence that ρ (mat) reflects at least qualitatively the properties of SWNT ropes (rather than being completely dominated by morphology) is provided by data from a 10- μ m-long sample consisting of straight defect-free rope segments interspersed with 1–2 μ m tangled regions, Fig. 3. In this sample, inter-rope contacts are no doubt required to ensure continuity between voltage probes, as in the mat samples, while the qualitative behavior of $\rho(T)$ is similar to the single rope and mat results, with $T^*\sim 250$ K.¹⁸ We thus believe the crossover phenomenon is an intrinsic feature of electron transport in the ropes, while the variability of T^* from sample to sample indicates that it is controlled by the different gross morphologies, defects and/or disorder.¹⁹

The positive $d\rho/dT$ at high temperature indicates that the SWNT ropes are the first nanotube material to exhibit this classic attribute of a metallic state, most likely because the effects of defects and disorder are less severe than in previ-

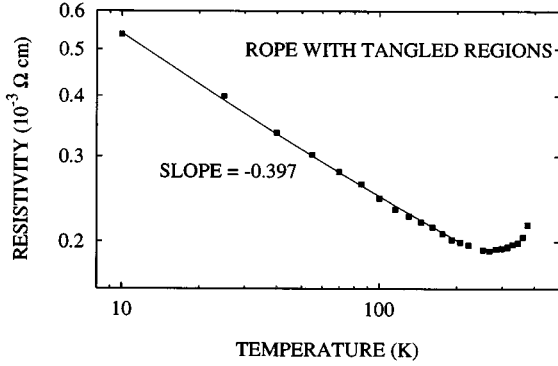


FIG. 3. Log-log plot of two-point ρ_{\parallel} vs T for a rope with tangled regions; absolute value is approximate due to uncertainties in rope diameter. Solid line is a power-law fit up to 200 K.

ous MWNT studies. This is of course consistent with the fact that the dominant SWNT in these samples is the (10,10) armchair tube which is predicted to be metallic. At first glance the quasilinear behavior suggests diffusive (phonon-limited) electron transport in the high- T limit of a Bloch-Grüneisen picture, in which the weak temperature dependence would be attributed to a relatively small net electron-phonon coupling. The carrier concentration and the density of states at the Fermi energy of (10,10) SWNT's are predicted to be small—scaling from a local-density-approximation calculation for the (5,5) case²⁰ we estimate $N(E_F) \sim 2/\text{eV}$ per 60 carbons (both spins), only 1/10 that of metallic K_3C_{60} (Ref. 21) which is already a low electron density system.²² For comparison, ρ_a of graphite exhibits a similarly weak and positive temperature derivative near 300 K (and no crossover to negative $d\rho/dT$), while the overall T dependence is more dramatic¹⁴ with $\rho(300\text{ K})/\rho(4\text{ K}) \sim 10$. On the other hand, given the energy scale of the relevant phonons, it is unlikely that the high- T limit would be reached at T as low as 50 K (cf. Fig. 2 for the single rope). Thus there may be some interesting new physics in the quasilinear $\rho(T)$ of SWNT ropes.

The negative $d\rho/dT$ at low T is harder to explain, absent more and different experimental information. Carrier freeze-out can be ruled out because, even if a gap opened at low T for some reason, the implied activation energy would be unphysically small.⁶ Figure 2 is reminiscent of Kondo alloys—the resistivity increase at low T could be due to spin-flip scattering from traces of Co and Ni incorporated in the SWNT, although it is hard to understand how the magnetic impurity density (measured by T^*) could vary so strongly among samples prepared from the same doped target, or by mechanical treatment. We cannot entirely rule out a T -dependent admixture of ρ_{\parallel} and ρ_{\perp} , for single ropes as well as mats, since we cannot be sure that we are making contact to all the tubes in a rope, and the length between voltage probes may not be sufficient to avoid the effect of intertube transport. On the other hand, it is far more typical for a high-resistivity tensor component to be corrupted by low-resistivity shorts, the inverse of the present case. Finally, the two-point and four-point resistivities are comparable, indicating that contact resistance is negligible.

The work of Langer *et al.* leads us to speculate as follows. The magnetoconductance of $\sim 200\text{-\AA}$ -diameter MWNT's below 100 K is interpreted in terms of 2D weak localization,⁴ the dimensionality being fixed by the large diameter, not by the coupling between concentric shells which is estimated to be only $\sim 1/10$ that of *ABAB* . . . stacked graphite due to the nonregistry of C atoms between adjacent tubes.¹⁴ Our ropes of 13.8-\AA -diameter SWNT's are more likely to be 1D since transport within a SWNT involves a single transverse channel⁹ and the coupling between six-coordinated SWNT's in a rope will be even weaker than the intershell coupling in MWNT's because neighbor tubes ‘‘touch’’ only along six lines, all of which cannot contain C atoms since the lattice symmetry is incompatible with the five-fold azimuthal symmetry of (10,10) tubes. The observed values of rope diameter and ρ_{\parallel} suggest that the Thouless criterion for 1D localization will be satisfied for $T < 20\text{--}40\text{ K}$,²³ assuming that ρ_{\parallel} is a measure of inelastic scattering and thus controls the cutoff length L_{Th} . This is consistent with $T^* \sim 35\text{ K}$ for a defect-free rope (Fig. 2). Phase coherence is maintained with increasing T until intertube hops become sufficiently frequent to destroy it. Above T^* the rope system becomes a normal anisotropic 3D metal, absent sufficient disorder to induce 3D localization.

Magnetoconductance would be an obvious experimental test of the above hypothesis.⁴ Another would be to determine if T^* is tunable by hydrostatic pressure; increased intertube overlap should shift the 1D \rightarrow 3D crossover to lower T . Long-wavelength bends of armchair SWNT's do not contribute to carrier backscattering, whereas even a modest twist, of order 1 complete revolution per 2 micrometers of length, introduces a gap of order 20 meV at E_F .⁹ A local fluctuation of this type would backscatter an electron, enhancing localization of the 1D wave function. Twisting the defect-free rope about its long axis should affect the low- T resistivity by shifting T^* and/or by changing the functional form of $\rho(T)$.²³ More challenging would be to measure $\rho(T)$ for a single defect-free SWNT; the much smaller characteristic dimension implies that 1D localization should survive to much higher T . Finally, the ropes appear to be long enough to search for scale-independent conductance, a definitive signature of localization in 1D.

While similar overall $\rho(T)$ behavior is observed in mats and single ropes, Fig. 2 suggests that $\langle \rho \rangle$ increases more rapidly with decreasing T than ρ_{\parallel} , raising the possibility of different low- T mechanisms. One possibility is that static disorder in tangled ropes induces weak 3D localization, which persists with increasing T until the dynamic disorder is sufficient to dephase the 3D wave function. The single rope in Figs. 1 and 2 has the least disorder, and its low T^* reflects the coherence limit of intrinsic 1D localization. Mats and defective ropes have higher T^* due to ‘‘excess’’ disorder from twists and tangles. Compressing the mat increases T^* slightly at first, which could be associated with partial crushing of tubes and ropes normal to the mat surface. Low-yield samples (and MWNT's) have T^* 's $> 300\text{ K}$; localized behavior persists to higher temperatures due to the increased defect density and disorder.

The weakly positive $d\rho/dT$ was anticipated in previous publications, where it was pointed out that weak electron-phonon coupling in a carbon nanotube would be insufficient

to stabilize a 1D Peierls distortion.⁷ A similar argument applies to superconductivity, which is unlikely to occur at high T_c in doped ropes. $N(E)$ is rather flat within ± 1 – 2 eV of the neutral tube E_F ,^{7,20} so we expect T_c 's in the mK range typical of the graphite intercalation compound KC_8 rather than the 20 K of K_3C_{60} , unless intercalation of a rope lattice shifts E_F by more than 1–2 eV or introduces new modes which couple strongly to electrons. On the other hand, prospects for highly conducting synthetic nanometals based on neutral and doped ropes are bright. It is hoped that the present results and speculations, and the availability of high-yield samples of well-characterized simple nanotube structures, will motivate further work—extending the resistivity

measurements to higher and lower T , galvanomagnetic experiments, electron and optical spectroscopies, and theory.

We are grateful for helpful conversations with C. L. Kane, E. J. Mele, and J. W. Mintmire, and the experimental assistance of Qiumin Lin. Work at Penn supported by the Department of Energy (DE-FC02-86ER45254) and by the National Science Foundation MRL Program (DMR91-20668). Work at Rice supported by the Office of Naval Research (N00014-91-J1794), the Advanced Technology Program of the State of Texas (003604-047), the National Science Foundation (DMR95-22251), and the Robert A. Welch Foundation (C-0689).

¹T. Ebbesen, *Phys. Today* **49**, 26 (1996).

²A. Zettl, *Adv. Mater.* **8**, 443 (1996).

³W. A. de Heer *et al.*, *Science* **268**, 845 (1995).

⁴L. Langer *et al.*, *Phys. Rev. Lett.* **76**, 479 (1996).

⁵H. Dai, E. W. Wong, and C. M. Lieber, *Science* **272**, 523 (1996).

⁶T. W. Ebbesen *et al.*, *Nature* **382**, 54 (1996).

⁷J. W. Mintmire, B. I. Dunlap, and C. T. White, *Phys. Rev. Lett.* **68**, 631 (1992).

⁸N. Hamada, S. Sawada, and A. Oshiyama, *Phys. Rev. Lett.* **68**, 1579 (1992).

⁹C. L. Kane and E. J. Mele, *Phys. Rev. Lett.* (to be published).

¹⁰T. Guo *et al.*, *Chem. Phys. Lett.* **243**, 49 (1995).

¹¹A. Thess *et al.*, *Science* **273**, 483 (1996).

¹²J. M. Cowley, P. Nikolaev, A. Thess, and R. E. Smalley, *Chem. Phys. Lett.* (to be published).

¹³A. M. Rao *et al.*, *Science* (to be published).

¹⁴J. R. Charlier and J.-P. Issi, *J. Phys. Chem. Solids* **57**, 957 (1996).

¹⁵Model R2205, MMR Technologies, Mountain View, CA 94043.

¹⁶Ordinarily the difference between oriented crystal and pressed powder pellet measurements depends not only on the intrinsic anisotropy of the resistivity tensor but also on the morphology of the powder and the nature of the interparticle contacts. Factors of several hundreds are obtained for a wide variety of materials if the pellets are pressed to within a factor ~ 2 of bulk density.

Were it not for the extreme aspect ratio of the “particles” in our “powder,” the extremely low density of the as-grown mats would imply a much greater factor difference.

¹⁷A rope length of 30 μm , not inconsistent with TEM, represents 1% of the distance between voltage probes.

¹⁸The high T^* and extended low- T range allows to extract a more reliable value for the exponent characterizing the negative $d\rho/dT$ regime, namely, -0.4 .

¹⁹Interestingly, similar behavior with $T^* \sim 40$ K and positive and negative slopes comparable to the rope results are observed for the c -axis resistivity of the stage-1 electron-doped graphite intercalation compound KC_8 [K. Phan, C. D. Fuerst, and J. E. Fischer, *Solid State Commun.* **44**, 1351 (1982)]; for the in-plane resistivity of the stage-1 hole-doped compound $\text{C}_{5.8}\text{F}$ [L. Piroux *et al.*, *Phys. Rev. B* **45**, 14 315 (1992)].

²⁰J. W. Mintmire, in *Electrical, Optical, and Magnetic Properties of Organic Solid State Materials*, MRS Symposia Proceedings No. 247, edited by L. Y. Chiang, A. F. Garito, and D. J. Sandman (Materials Research Society, Pittsburgh, 1992), p. 339.

²¹W. H. Wong *et al.*, *Europhys. Lett.* **18**, 79 (1992).

²²Y. J. Uemura, L. P. Le, and G. M. Luke, *Synth. Met.* **56**, 2845 (1993).

²³D. J. Thouless, *Phys. Rev. Lett.* **39**, 1167 (1977); P. A. Lee and T. V. Ramakrishnan, *Rev. Mod. Phys.* **57**, 287 (1985).